X-ray Coherent Diffraction Imaging of Nanomaterials

Ross Harder & Ian K Robinson

May 1, 2013

Abstract

The last decade has seen a remarkable surge in x-ray characterization methods[1]. Imaging with x-rays has evolved from simple radiography, to image internal structure and diagnose injury, to a full fledged tool for nanoscale characterization[2]. Central to this development has been the advent of high brilliance synchrotron and free electron laser sources of X-rays. The high degree of spacial coherence of the resulting beams has enabled novel new imaging methods. Of these, Coherent Diffraction Imaging (CDI) has proven highly successful at imaging structure in nano materials[3]. In addition, this imaging method can be combined with Bragg diffraction (BCDI) to image strain with high sensitivity[4, 5].

Since the discovery of X-rays by Röntgen in 1895[6] the penetrating power and short wavelength of this form of light has been exploited in many ways. Indeed, the term x-ray has even become synonymous with the radiography images that are commonplace in medicine to non invasively diagnose

injury and disease. Perhaps less common in everyday experience is the concept of diffraction of x-rays by periodic structures such a crystals. This phenomenon was discovered by the father-son team of W.H. and W.L. Bragg in 1913 [7, 8] and has contributed tremendously to society, even though one seldom encounters Bragg's diffraction spots on a daily basis.

Bragg diffraction arises due to the extremely short wavelength of x-ray light. X-rays have wavelengths similar to the spacing between atomic planes within a crystal. It is possible to orient a crystal in such a way that x-ray beams reflected from individual lattice planes can constructively add up in relative phase, via exactly the same mechanism that gives rise to maxima and minima in the classical Young's double slit experiment. With such an alignment one can observe extremely bright reflected x-ray beams (Bragg beams) from specific orientations of the crystal lattice. When the alignment condition is not carefully met, the incident beam will pass through the sample or be simply absorbed in the form of heat. This behavior is fundamentally different than reflection of visible light by a mirror, as that reflected intensity is relatively insensitive to the angle. The very nature of Bragg diffraction means that it has exquisite sensitivity to the atomic structure of matter. It is this powerful capability that has allowed the determination of the atomic structure of everything from the genetic building blocks of life[9] to advanced materials for efficient lighting[10].

Radiography and diffraction are in some sense the opposite ends of the spectrum for structural studies of matter. While the diffraction condition gives average atomic scale information of the sample, radiography gives images of local structure in the micro-millimeter length scales. Quite often local

structure has a profound impact on the properties of the material. This is particularly evident within nano materials, or objects having spacial dimensions of a few hundreds of nanometers or less. As pointed out in Robinson et al. [5], the unique properties of these materials require innovative new tools to study them. Especially when one needs to study these materials in their native setting, or within complex or corrosive environments.

To study the local structure of materials at spatial resolution better than 1 μm the x-ray equivalent of a microscope is a powerful tool[11]. The foundation of high resolution x-ray microscopy is the x-ray Fresnel Zone Plate (FZP) lens. Due to the weak interaction of the x-rays with matter, a diffractive optic like an FZP is ideal. Currently the best FZPs designed for hard x-ray (short wavelength) use are reaching down to 20 nm resolution[12]. There are substantial technical challenges in producing diffractive lenses with smaller features sizes and hence higher resolution. Actually, the current record for focussing hard x-rays goes to a mirror system which produced a 7 nm focused x-ray beam[13]. Both mirror and diffractive x-ray lenses are technologically challenging and as with optical microscopy, high resolution comes at the cost of working distance of the lens. In the case of x-ray microscopy, this cost is quite high as the one of the greatest benefits of hard x-rays, in particular, is their greater penetration into both materials and environments[2, 14].

When one wishes to study a sample within an environmental cell, or needs information at resolutions beyond that of the best x-ray lenes, the lens of the microscope can be replaced with computational algorithms. This method, known as Coherent Diffractive Imaging (CDI), exploits the bril-

liance of modern synchrotrons and free electron lasers[15] to image materials at potentially very high spatial[16, 17], and now temporal, resolution[18]. The reason the method can image local structure, even without a lens, is that the beam itself has a point to point phase correlation that is preserved throughout the interaction with the sample. The x-rays scattered from different regions of the sample reach a camera with a fixed relative phase to each other and constructively or destructively interfere accordingly. So while not formally identical to the diffraction from crystal planes that Bragg originally described, the fact that interference of waves scattered from different regions of the sample is what is measured, makes the name appropriate. Essentially the squared modulus of the Fourier Transform of the structure of the sample is measured at the detector plane. As a result ,CDI is subject to an obstacle similar to the phase problem of x-ray crystallography[19, 20]. The key to producing an image from the measured data, which bears little obvious resemblance to the sample, it to computationally retrieve the phases of the scattered waves and propagate, via Fourier Transform, back to the plane of the sample[21, 22, 23].

The resolution of CDI is determined in a similar way to lens based microscopy. While the microscope resolution is determined by the numerical aperture (NA) of the lens, the CDI resolution is determined by the numerical aperture of the data, or to what angle the x-rays are scattered by the sample. In the language of diffraction, it is the maximum momentum transfer imparted to the scattered beam that determines the resolution of the data, and hence the resolution of the obtained image.

The dominate scattering mechanism, or contrast, is the electron density

4

of the material. Coherent imaging can possesses remarkable sensitivity to material properties. In Diaz et al. they illustrate a 2% accuracy in determination of the density of SiO_2 microspheres [24]. Coherent imaging is being developed to exploit a variety of other contrast mechanisms. Linear dichroism in magnetic systems has already been used to image labyrinth domains in GdFe films[25] and instrumentation to exploit circular magnetic dichroism as an imaging contrast is being developed. In addition, coherent imaging can be combined with the exquisite sensitivity of x-rays to distortions of a crystalline lattice to image strain. Usually referred to as Bragg Coherent Diffractive Imaging (BCDI), the ability to image strain on the nanometer scale in three dimensions is highly novel.

Coherent imaging is currently done in two somewhat distinct modes. The original method relies on the sample being compact in space, or smaller than the coherent x-ray beam in which it is measured[21, 3]. This is traditionally what we call CDI. The measurement can be done either in the small angle geometry, where the scattered x-rays lye near the direct beam, or in the vicinity of Bragg peaks of crystals, where the sample is, of course, a crystal and the detector and sample are oriented at a Bragg condition of the lattice[4, 5]. The most recent addition to coherent imaging methods has been generally called Ptychography, or Scanning X-ray Diffractive Imaging[26, 27]. The goal of this method is to remove the requirement that the sample be compact. Ptychography can image, with all of the benefits of greater working distance and potentially higher resolution, an extended field of view in a sample of larger size. The root of the word ptychography is from Greek meaning to fold, and that is the principle behind the method.

The phase retrieval process of CDI is not very robust when the object is not compact, or finite in extent. To overcome this technical difficulty the beam is scanned across the sample and measurements are done at overlapping locations. This folding of the measurements from overlapping regions of the sample greatly aide in the phase retrieval process to produce the image of the sample.

In recent years the phase retrieval algorithms have been the greatest area of development in the field. For CDI, they are still primarily based on the iterative algorithms of Gerchberg and Saxton, which were developed for the case of two measurements. One done in diffraction space, identical to CDI, and another done in direct, or image, space, where with an electron microscope one can switch at the push of a button. The algorithms are iterative in nature, using a computational tool known as the Fast Fourier Transform (FFT) to switch back and forth between the two measurement spaces. The FFT is in its own right a topic of research among computer scientists, but thankfully there canned libraries which are reasonably robust. In the Gerchberg and Saxton case they were attempting to improve the resolution of the images formed in an electron microscope. In the CDI case we have only one measurement in the diffraction space. The algorithms coined Hybrid Input-Output (HIO) and Error Reductions (ER) were defined in Fienup's 1982 paper and are the true workhorses of CDI. For CDI, since there is no measurement in direct space, we must encode as much information as we have regarding the sample to aide the phase retrieval algorithm in convergence. Typically the size of the sample is encoded in the support constraint that determines how the electron density of the image is modified at each iteration.

A formulation by Marchesini et al. called Shrinkwrap allows for the support size to be automatically determined as the iterations of the algorithm proceed[28]. Chen et al. developed a method to improve the reliability of an image called Guided-HIO. In GHIO multiple sequences of phase retrieval are started from random distributions and the resulting images from each are combined together periodically during the iterations, in a variety of ways, to converge to a single solution[29]. One of the most recent additions to the iterative algorithms has been the ability to correct for imperfect coherence in the x-ray beam[23]. This can arise as a consequence of the beam line configuration (slits opened too wide) or scatter from windows that the x-ray beam must pass through. Poor coherence in the beam reduces the contrast in the bright and dark regions of the diffraction pattern. In direct space, the density recovered will typically be less uniform. This method was critical for application of BCDI to a sample within a high pressure diamond anvil cell [30]. Due to the presence of a gasket that was traversed by the beam both entering and exiting the cell, the partial coherence of the incident beam became more severely intertwined[14].

In this text we describe an example of coherent imaging of a nanometer scale crystal of Barium Titanate mounted on a thick substrate of silicon. In this example the compact nature of the sample is taken into account during the phase retrieval process to produce an image. Since this measurement was done in the vicinity of a (110) Bragg peak of the crystal we were sensitive to distortions of the lattice of the crystal due to strain. Intuitively the strain sensitivity comes from the fact that different positions in the crystal will have slightly different lattice spacing and hence diffract x-rays to minutely

different angles. Due to the coherence of the beam this fact will be encoded in the interference pattern produced in the near vicinity of the Bragg peak. By the nature of Fourier Transforms, upon computational phase retrieval, the image will be of a complex (containing both real and imaginary parts) density distribution within the object. The amplitude of the complex numbers is directly proportional to the electron density of the crystal, while the phase of the complex numbers is directly related to the distortion of the lattice along the direction of the crystal planes which are aligned at the Bragg condition.

Fig. 1 illustrates the BCDI experiment at the Advanced Photon Source (APS) at Argonne National Laboratory. At this synchrotron beamline the coherent fraction of the synchrotron source is our primary concern. Precision slits are almost the only optical components that touch the beam. The instrument does contain a monochromator, which is a pair of Silicon (111) oriented crystals, to select just a single wavelength of x-rays from the spectrum produced by the synchrotron. These crystals are carefully polished to maintain the purity of the coherent wavefront. After the monochromator there is a precision slit that selects just a single coherent mode from the beam and a Kirk-Patrick Baez mirror system that focuses the x-ray beam from tens of micrometers down to less than one micrometer[31]. Again, this focusing optic does not determine the final resolution of the image, it is simply used to concentrate as much of the coherent beam onto a tiny sample as possible. It has a long working distance, in x-ray lens terms, of 7cm or more, leaving room for temperature stages, gas environments, high pressure cells or any other in-situ action the scientist can conceive of.

Nanosized Barium Titanate (BTO) is an important industrial material for making supercapacitors. BTOs dielectric constant peaks as a function of size with a maximum around 140nm with a factor of 3 enhancement of dielectric constant resulting in a big improvement in capacitor performance [32]. A major industry is currently building up for energy storage, which is of significant interest in Basic Energy Sciences.

The structural origin of the dielectric enhancement in nanometer-sizes crystals of BTO is an important scientific question which can be addressed by Bragg Coherent X-ray Diffraction Imaging (BCDI). The dielectric susceptibility, the amount of electric polarization for a given applied field, is a structural quantity related to the degree of ionic displacements allowed in a given lattice. The ions are expected to have fixed charges, so the polarization is directly proportional to the lattice distortion. Nanoparticles have a large surface-to-volume ratio so can presumably take advantage of addition degrees of structural freedom at their surfaces, which in turn allows a higher polarization. The question of how the electric polarization is distributed within the nanoparticle demands three dimensional spatial imaging of the crystals distortions, as BCDI can provide.

BTO has a classical perovskite structure, for which the parent phase (above 100C at ambient pressure) is cubic, becoming tetragonal at room temperature [33]. This phase transition is influenced by pressure and also by particle size which results in effective pressure [34]. The dielectric polarization, which results from oxygen ion displacements in the opposite direction from the Ba and Ti cations, is present in all phases [35]. A recent publication used X-ray powder diffraction analysis to infer a core-shell structure

for the nanocrystalline BTO[36]. The experiments used Rietveld refinement to fit the splitting of the Bragg peaks observed for a range of particle sizes to determine the ratio of tetragonal and cubic material in the sample. The core-shell picture, in which the core is tetragonal and the shell is cubic, was proposed to explain the size-dependence of those ratios. This core-shell model, which could explain the enhancement of dielectric constant, can be imaged directly by BCDI without the need to invoke models.

BCDI is a well established technique at the APS [5] which is able to image nanometer-sized crystals in 3D with a resolution of 30nm or better. Strains are detected as phase in the direct-space images, and can be quantitatively analyzed as projections of the local displacements onto the scattering Q-vector. The tetragonal/cubic core shell structure would therefore show up as a broadening of the cubic-index Bragg peaks, translating into characteristic phase patterns of the 3D images of the crystals. We have previously observed core-shell strain structures on micron-sized zeolite crystals [37].

BCDI has been found to be effective in looking at twinning in complex oxide crystals [38]. Merohedrally twinned crystals have two (or more) orientations of crystal grains which are joined at a common interface located at one of the crystallographic planes. The crystallographic description is complicated in general by the presence of two lattices, but the Generalized Phase Approximation (GPA) [39] can be used to represent one lattice as a distortion of the other [35]. The second crystal is considered to have complex electron density in which its local orientation is represented as a phase at every point in space. Using the GPA, the second crystal acquires a phase ramp when described in the coordinate system of the first crystal of the

twin [38]. In this way, the tetragonal-cubic core-shell structure proposed by Hoshina[36] will be identified as a flat phase in the interior (tetragonal reference lattice) with phase ramp structures on the outside representing the cubic crystallographic phase, which appears as a distortion.

In this case the sample consists of a silicon wafer which has been sprinkled with BTO nano crystals. The sample was mounted at the center of the diffractometer at beamline 34-ID-C of APS and the detector was placed at the nominal Bragg angle for BTO (110). Since many hundreds of crystals are in the x-ray beam at any given position of the sample, it was quite easy to find a Bragg diffraction beam from an individual nanocrystal like the one shown in Fig. 1. To measure the entire coherent diffraction pattern in the vicinity of the Bragg beam the crystal is rotated in direct space to translate the 3D coherent diffraction pattern in reciprocal space through the area detector. This particular crystal was rotated through XX degrees in steps of XX and individual slices of the 3D pattern were recorded. The individual slices of the 3D diffraction pattern were then stacked together to be fed into the phase retrieval programs.

We investigated the structures of 320 nm and 240 nm BTO crystals using BCDI. The diffraction patterns in Fig. 1 shows a clear fringed diffraction pattern from the facets of the 320nm crystal. Images of the 320 nm crystal in Fig. 2a&b show strains localized at two of the facets of the crystal shape. Fig. 2c shows a slice through the phase of the three dimensional density. The slice shows an interior that is a relative flat phase, except for one small region where the density appears missing. The phase here indicates the possible presence of a defect in the lattice that induces a dipole like distortion

field in the lattice, given by the opposite shade phase on either side of the position. The density here is not actually missing, but the lattice is sufficiently distorted that some of the phase contrast in direct space has caused on interference and reduced the amplitude of the complex density. In Fig. 3 a similar set of images are shown of the 240nm crystal. The phase-isosurface images show greatest strains on the top and bottom of the crystal, relative o the Q vector of the 110 Bragg peak. As in the larger crystal, the interior is relatively flat phase. There is an obvious scallop pattern shown in the phase slice, but this is likely structure below the resolution of the image and hence not reliable. These images indicate a pattern of strain in the particles which might be consistent with the core-shell model.

Coherent Diffraction Imaging is rapidly establishing itself at third and forth generation x-ray light sources like the Advanced Photon Source at Argonne National Laboratory and the Linac Coherent Light Source at Stanford Linear Accelerator, both of which are examples of National User Facilities (www.nufo.org). The imaging method is highly dependent on these high brilliance sources to produce the coherent beams. Dedicated instrumentation exists at these facilities and is supported by professional staff to run experiments with visitors. The reader should be aware that these capabilities are available to scientists with all levels of x-ray imaging background. Generally the national user facilities operate through a proposal review process that scores and prioritizes experiments to be done at each of the instruments. For the novice user, the instrument staff are generally very helpful in all stages of the proposal process and all are encouraged to engage these facilities in their research.

References

[1] Philip Willmott. An Introduction to Synchrotron Radiation. pages i–xv. John Wiley & Sons, Ltd, 2011.

[2] Martin Holt, Ross Harder, Robert Winarski, and Volker Rose. Nanoscale Hard X-Ray Microscopy Methods for Materials Studies. *Annu. Rev. Mater. Res.*, January 2013.

[3] Jianwei Miao, Pambos Charalambous, Janos Kirz, and David Sayre. Extending the methodology of X-ray crystallography to allow imaging of micrometre-sized non-crystalline specimens. *Nature*, 400(6):342–344, July 1999.

[4] Mark A Pfeifer, Garth J Williams, Ivan A Vartanyants, Ross Harder, and Ian K Robinson. Three-dimensional mapping of a deformation field inside a nanocrystal. *Nature*, 442(7098):63–66, July 2006.

[5] Ian Robinson and Ross Harder. Coherent X-ray diffraction imaging of strain at the nanoscale. *Nat Mater*, 8(4):291–298, April 2009.

[6] W K Röntgen. A New Form of Radiation. *Science, New Series*, 3(72):726–729, May 1896.

[7] W H Bragg and W L Bragg. The reflection of X-rays by crystals. *Proceedings of the Royal Society of London. Series A*, 88(605):428–438, 1913.

[8] W L Bragg. The structure of some crystals as indicated by their diffraction of X-rays. *Proceedings of the Royal Society of London. Series A*, 89(610):248–277, 1913.

[9] J D Watson and F H C Crick. A structure for deoxyribose nucleic acid. *Nature*, 171:737–738, 1953.

[10] H Amano, N Sawaki, I Akasaki, and Y Toyoda. Metalorganic vapor phase epitaxial growth of a high quality GaN film using an AlN buffer layer. *Applied Physics Letters*, 48(5):353, 1986.

[11] Yu-Tung Chen, Tsung-Nan Lo, Yong S Chu, Jaemock Yi, Chi-Jen Liu, Jun-Yue Wang, Cheng-Liang Wang, Chen-Wei Chiu, Tzu-En Hua, Yeukuang Hwu, Qun Shen, Gung-Chian Yin, Keng S Liang, Hong-Ming Lin, Jung Ho Je, and Giorgio Margaritondo. Full-field hard x-ray microscopy below 30 nm: a challenging nanofabrication achievement. *Nanotechnology*, 19(39):395302, August 2008.

[12] Joan Vila-Comamala, Yongsheng Pan, Jeffrey J Lombardo, William M Harris, Wilson K S Chiu, Christian David, and Yuxin Wang. Zone-doubled Fresnel zone plates for high-resolution hard X-ray full-field transmission microscopy. *Journal of Synchrotron Radiation*, 19(5):705–709, July 2012.

[13] Hidekazu Mimura, Soichiro Handa, Takashi Kimura, Hirokatsu Yumoto, Daisuke Yamakawa, Hikaru Yokoyama, Satoshi Matsuyama, Kouji Inagaki, Kazuya Yamamura, Yasuhisa Sano, Kenji Tamasaku, Yoshinori Nishino, Makina Yabashi, Tetsuya Ishikawa, and Kazuto Ya-

mauchi. Breaking the 10nm barrier in hard-X-ray focusing. *Nature Physics*, 6(2):122–125, November 2009.

[14] Wenge Yang, Xiaojing Huang, Ross Harder, Jesse N Clark, Ian K Robinson, and Ho-kwang Mao. Coherent diffraction imaging of nanoscale strain evolution in a single crystal under high pressure. *Nature Communications*, 4:1680–, April 2013.

[15] I A Vartanyants and A Singer. Coherence properties of hard x-ray synchrotron sources and x-ray free-electron lasers. *New Journal of Physics*, 12(3):035004.

[16] Yukio Takahashi, Nobuyuki Zettsu, Yoshinori Nishino, Ryosuke Tsutsumi, Eiichiro Matsubara, Tetsuya Ishikawa, and Kazuto Yamauchi. Three-Dimensional Electron Density Mapping of Shape-Controlled Nanoparticle by Focused Hard X-ray Diffraction Microscopy. *Nano letters*, 10(5):1922–1926, 2010.

[17] Yukio Takahashi, Yoshinori Nishino, Ryosuke Tsutsumi, Hideto Kubo, Hayato Furukawa, Hidekazu Mimura, Satoshi Matsuyama, Nobuyuki Zettsu, Eiichiro Matsubara, Tetsuya Ishikawa, and Kazuto Yamauchi. High-resolution diffraction microscopy using the plane-wave field of a nearly diffraction limited focused x-ray beam. *Physical Review B*, 80(5):054103, 2009.

[18] K Gaffney and H Chapman. Imaging Atomic Structure and Dynamics with Ultrafast X-ray Scattering. *Science*, 316(5830):1444–1448, 2007.

[19] D Sayre. The squaring method: a new method for phase determination. *Acta crystallographica*, 5(1):60–65, January 1952.

[20] J Karle and H Hauptman. The phases and magnitudes of the structure factors. *Acta crystallographica*, 3(3):181–187, May 1950.

[21] J Fienup. Phase retrieval algorithms: a comparison. *Applied optics*, 21(15):2758–2769, 1982.

[22] Ross Harder, M Liang, Y Sun, Y Xia, and I K Robinson. Imaging of complex density in silver nanocubes by coherent x-ray diffraction. *New Journal of Physics*, 12(3):035019, March 2010.

[23] J N Clark, X Huang, R Harder, and I K Robinson. High-resolution three-dimensional partially coherent diffraction imaging. *Nature Communications*, 3:993–, August 2012.

[24] Ana Diaz, Pavel Trtik, Manuel Guizar-Sicairos, Andreas Menzel, Pierre Thibault, and Oliver Bunk. Quantitative x-ray phase nanotomography. *Physical Review B*, 85(2):020104 EP–, 2012.

[25] A Tripathi, J Mohanty, S H Dietze, O G Shpyrko, E Shipton, E E Fullerton, S S Kim, and I McNulty. Dichroic coherent diffractive imaging. *Proceedings of the National Academy of Sciences*, 108(33):13393–13398, August 2011.

[26] J Rodenburg, A Hurst, A Cullis, B Dobson, F Pfeiffer, O Bunk, C David, K Jefimovs, and I Johnson. Hard-X-Ray Lensless Imaging of Extended Objects. *Physical review letters*, 98(3):034801, January 2007.

[27] Pierre Thibault, Martin Dierolf, Andreas Menzel, Oliver Bunk, Christian David, and Franz Pfeiffer. High-Resolution Scanning X-ray Diffraction Microscopy. *Science*, 321(5887):379–382, 2008.

[28] S Marchesini, H He, H Chapman, S Hau-Riege, A Noy, M Howells, U Weierstall, and J Spence. X-ray image reconstruction from a diffraction pattern alone. *Physical Review B*, 68(14):140101, 2003.

[29] Chien-Chun Chen, Jianwei Miao, Cheng-Liang Wang, and Ting-Kuo Lee. Application of optimization technique to noncrystalline x-ray diffraction microscopy: Guided hybrid input-output method. *Physical Review B*, 76(6):064113, 2007.

[30] H-K Mao, J Xu, V V Struzhkin, J Shu, R J Hemley, W Sturhahn, M Y Hu, E E Alp, L Vocadlo, D Alfe, G D Price, M J Gillan, M Schwoerer-Böhning, D Häusermann, P Eng, G Shen, H Giefers, R Lübbers, and G Wortmann. Phonon Density of States of Iron up to 153 Gigapascals. *Science*, 292(5518):914–916, January 2001.

[31] Malcolm R Howells, Daniela Cambie, Robert M Duarte, Steven Irick, Alasdair A MacDowell, Howard A Padmore, Timothy R Renner, Seungyu Rah, and Reubin Sandler. Theory and practice of elliptically bent x-ray mirrors. *Optical Engineering*, 39(10):2748–2762, October 2000.

[32] G Arlt, D Hennings, and G de With. Dielectric properties of fine-grained barium titanate ceramics. *Journal of Applied Physics*, 58(4):1619–1625, January 1985.

[33] Gen Shirane and Kazuo Suzuki. On the Phase Transition in Barium-Lead Titanate (1). *Journal of the Physical Society of Japan*, 6(4):274–278, April 1951.

[34] Ian Robinson. Nanoparticle Structure by Coherent X-ray Diffraction. *Journal of the Physical Society of Japan*, 82(2):021012, December 2012.

[35] G Shirane, B Frazer, V Minkiewicz, J Leake, and A Linz. Soft Optic Modes in Barium Titanate. *Phys. Rev. Lett.*, 19(5):234–235, July 1967.

[36] Takuya Hoshina, Satoshi Wada, Yoshihiro Kuroiwa, and Takaaki Tsurumi. Composite structure and size effect of barium titanate nanoparticles. *Applied Physics Letters*, 93(19):192914, 2008.

[37] Wonsuk Cha and et al. Core-Shell Strain Structure of Zeolite Microcrystals.

[38] Miguel A G Aranda, Felisa Berenguer, Richard J Bean, Xiaowen Shi, Gang Xiong, Stephen P Collins, Colin Nave, and Ian K Robinson. Coherent X-ray diffraction investigation of twinned microcrystals. *Journal of Synchrotron Radiation*, 17(6):751–760, October 2010.

[39] Martin Hÿtch, Florent Houdellier, Florian Hüe, and Etienne Snoeck. Nanoscale holographic interferometry for strain measurements in electronic devices. *Nature*, 453(7198):1086–1089, June 2008.
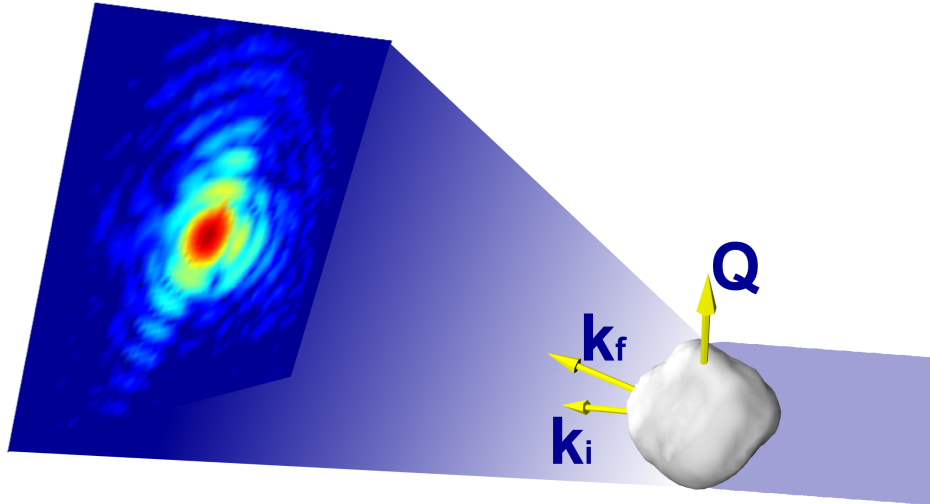
Figure 1: Illustration of the BCDI experiment at APS 34-ID-C. The 320nm diameter Barium Titanate crystal is aligned at the 110 Bragg angle at the center of the diffractometer. A slice through the three dimensional coherent diffraction pattern is measured in the far field at the Bragg angle indicated by the direction of the arrow labeled $\mathbf{k_f}$. The difference between the incident momentum vector $\mathbf{k_i}$ and $\mathbf{k_f}$ is given by the arrow labeled $\mathbf{Q}$. It is the direction of $\mathbf{Q}$ onto which the distortions of the crystal lattice are projected in our BCDI images and is the so called reciprocal lattice vector that defines the Bragg condition.
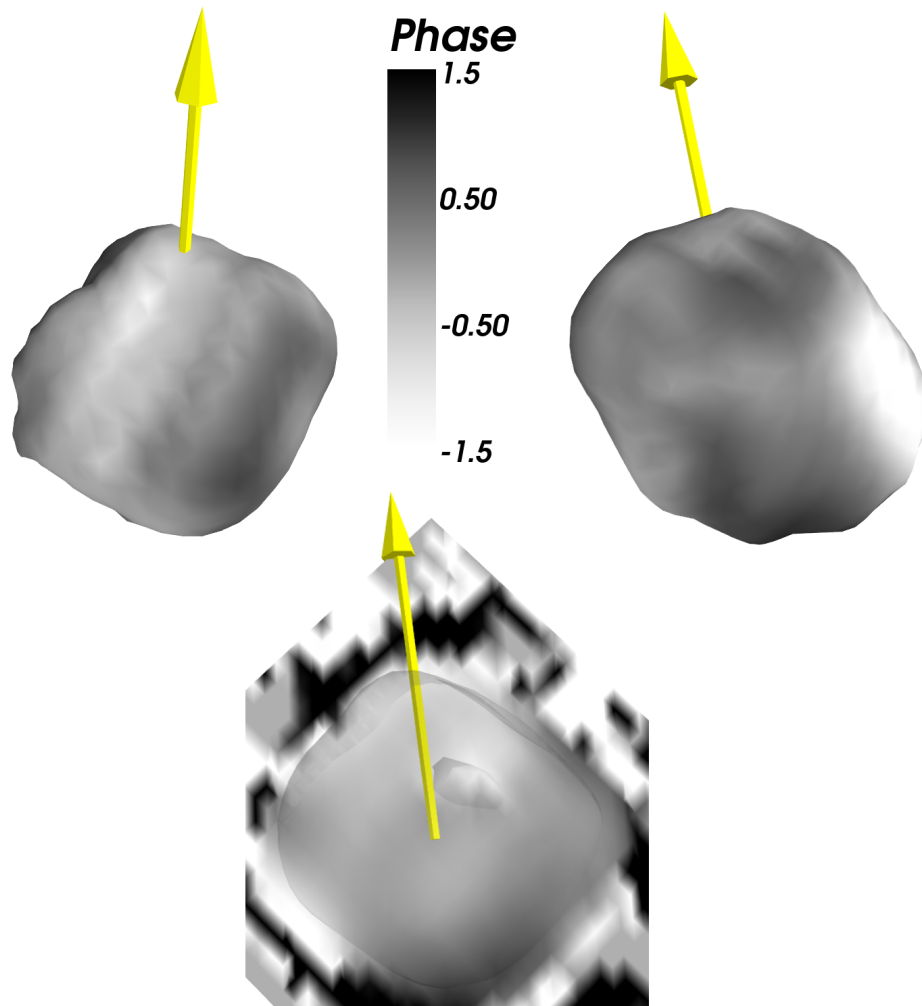
Figure 2: Views of opposite sides of the 320nm diameter BTO crystal shown in Fig. 1 produced from the tetragonal-sensitive 110 Bragg peak. The three dimensional contour, or isosurface, is at the 25% level. The shading on the surface is determined by the phase of the density, or distortion of the lattice, at a given position. The total range in phase, from -1.5 to +1.5 radians, corresponds to approximately one half of the 110 lattice spacing, or 2.8 angstroms of accumulated displacement along the direction indicated by the **Q** vector in the illustration. The phase of the interior is seen on the slice through phase of the 3D volume. The randomized phases outside of the semitransparent isosurface can be disregarded.
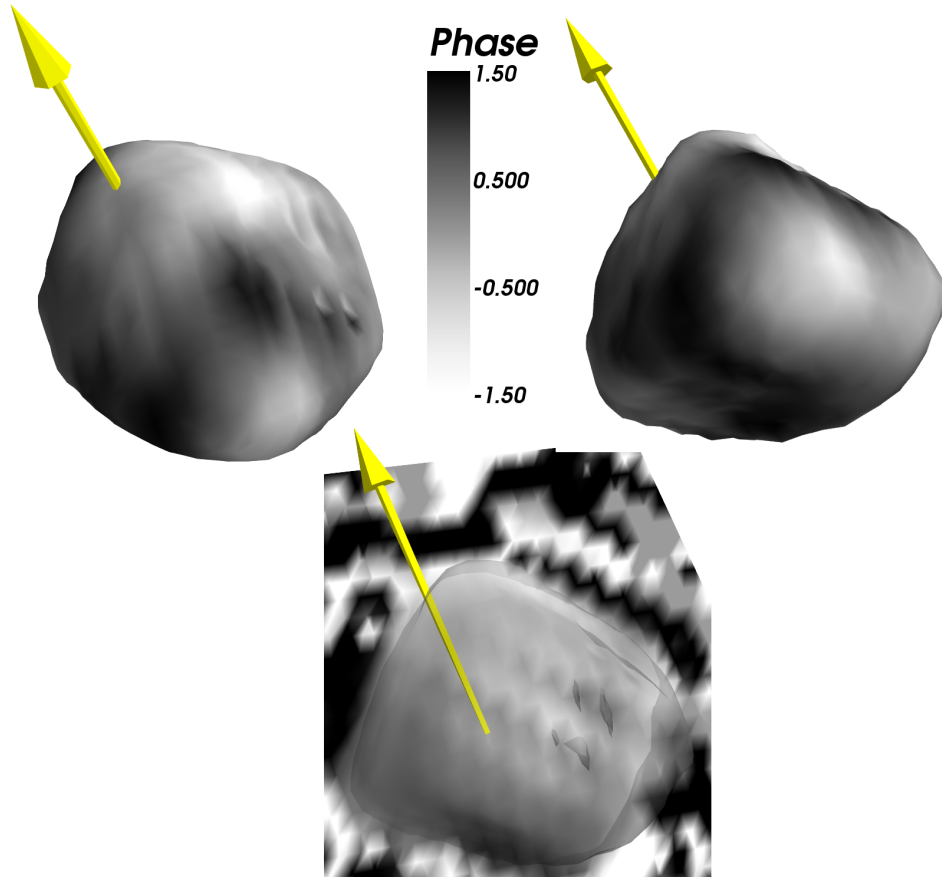
Figure 3: Views showing the top and bottom of a phase-isosurface of another BTO crystal with a diameter of about 240nm. The arrow indicates the direction of the reciprocal lattice vector onto which the distortion of the lattice is projected. In (c) a slice through the phase of the complex image is shown cutting through a semitransparent isosurface in the amplitude. The phase of the interior is relatively flat relative to the outer edges where dark and light regions are obvious.